35th Annual International Conference of the IEEE EMBS
Osaka, Japan, 3 - 7 July, 2013

Temporal Resolution of Nanopore Sensor Recordings

Jacob K. Rosenstein, *Member, IEEE* and Kenneth L. Shepard, *Fellow, IEEE*

***Abstract*—Here we discuss the limits to temporal resolution in nanopore sensor recordings, which arise from considerations of both small-signal frequency response and accumulated noise power. Nanopore sensors have strong similarities to patch-clamp ion channel recordings, except that the magnitudes of many physical parameters are substantially different. We will present examples from our recent work developing high-speed nanopore sensing platforms, in which we physically integrated nanopores with custom low-noise complementary metal-oxide-semiconductor (CMOS) circuitry. Close physical proximity of the sensor and amplifier electronics can reduce parasitic capacitances, improving both the signal-to-noise ratio and the effective temporal resolution of the recordings.**

I. Introduction

Nanopore sensors have attracted considerable attention as single-molecule non-optical sensors for DNA sequencing and other applications, but their performance is often constrained by low signal-to-noise ratios [1, 2]. This generally manifests itself as a tradeoff between the noise amplitude and temporal resolution of a recording. Analyte molecules can travel through nanopores in mere nanoseconds, but the time resolution of most nanopore recordings has commonly been limited to no faster than tens of microseconds.

Here we review the factors that determine signal-to-noise ratios in nanopore sensor recordings and discuss their temporal resolution limits. This discussion shares many similarities with considerations for patch-clamp recordings of single ion channels [3]. However, as the relevant physical parameters can be quite different, it is useful to revisit these topics specifically for nanopore sensors. In recent work, we have shown that by designing a custom low-noise integrated circuit amplifier and reducing parasitic capacitances, nanopore signals as brief as one microsecond can be resolved [4]. We will review the conclusions of this work and discuss the potential for future improvements in time-resolved nanopore sensing.

II. Electronic Properties of Nanopore Sensors

Nanopore sensors consist of a nanoscale aperture in a thin membrane separating two isolated electrolytes (referred to as *cis* and *trans*). The nanopore forms a nanoscale junction that allows ions to pass between the two electrolytes. Generally a static voltage bias is applied between the two chambers, creating an electric field near the nanopore which attracts charged analyte molecules. Single molecules are detected by changes in the ionic current while a molecule is present in the nanopore.

J.K.R. is an Assistant Professor of Engineering at Brown University, Providence, RI, USA. (phone: 401-863-2652; e-mail: jacob_rosenstein@brown.edu).

K.L.S. is a Professor of Electrical Engineering and Biomedical Engineering at Columbia University, New York, NY, USA. (e-mail: shepard@ee.columbia.edu).

Nanopore sensors can be constructed in a variety of ways, with one main classification being between those nanopore sensors based on biological ion channel proteins and those fabricated in solid-state materials. The first nanopore demonstration was made with a single alpha-Hemolysin (α-HL) protein reconstituted into a lipid bilayer [5], and α-HL continues to be the most popular biological nanopore. Solid-state nanopores in a variety of different materials have also been demonstrated [6], and perhaps the most-utilized to date are solid-state nanopores drilled through dielectric membranes with a transmission electron microscope [7].

A. Measurable Current Signals

The simplest model for a nanopore is a cylindrical channel of diameter d through a membrane of thickness h, whose ionic resistance (R_P) or conductance (G_P) can be described by:

$$R_P = \frac{1}{G_P} = \frac{4h}{\pi d^2 \mu n q} \quad (1)$$

where μ is the mean electrophoretic mobility of the ions in the electrolyte, n is the number density of ions, and q is the elementary charge.

In common high-salt conditions analyte molecules temporarily reduce the pore conductance, and thus the steady-state bias current determines the maximum possible signal level. α-HL nanopores have a conductance (G_P) of approximately 1 nS in 1M KCl; therefore, at a voltage bias of 100 mV they can produce maximum signal currents on the order of 100 pA. Solid-state nanopores typically have larger diameters and correspondingly larger signal currents. For example, a 4-nm diameter nanopore in a sub-10nm-thick silicon nitride nanopore can have a conductance of 23 nS in 1M KCl, producing signals larger than 4 nA [8].

The duration of signals measured with nanopore sensors is related to the time that a single analyte molecule occupies the pore. This can either be a function of the velocity of a freely moving molecule, or it can be related to the time constant of a chemical reaction, such as the adsorption of a molecule to the pore or the breaking of a chemical bond. Signals from nanopore recordings thus span timescales from the several hours it may take for a single experiment, down to the nanosecond timescales of free diffusion of a molecule through a pore.

B. Voltage-Clamp Amplifiers

Although nanopores can produce signals that vary in amplitude and duration over several orders of magnitude, they are usually all measured using the same tools. Primary among these instruments is the voltage-clamp current amplifier, adopted from electrophysiology platforms for its low-noise and high-bandwidth properties [3].

978-1-4577-0216-7/13/$26.00 ©2013 IEEE

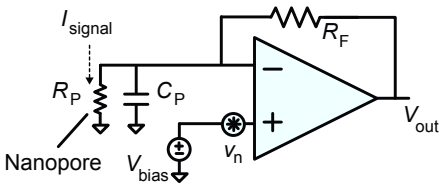

Figure 1: Simplified circuit schematic of a nanopore voltage-clamp current recording

A voltage-clamp measurement uses an operational amplifier to regulate the voltage across the nanopore by applying a variable current through a negative feedback loop. The current through the nanopore is measured by relating the output voltage of the amplifier through the transimpedance of the feedback network. In an ideal scenario, the output voltage has a simple linear relationship to the nanopore current, but in practical experiments there are important considerations of instrument noise.

The primary parasitic elements in nanopore measurements are capacitances associated with the nanopore's supporting membrane, electronic interconnects, and the input of the amplifier itself. These capacitances do not directly limit the bandwidth of a measurement. However, in extreme cases they can result in amplifier feedback instability, and in all cases parasitic capacitances will introduce measurement noise. Fig. 2 illustrates the important frequency regimes of noise power in a nanopore voltage-clamp recording.

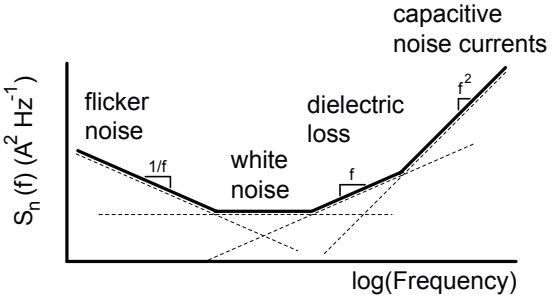

Figure 2: Illustrated noise spectral density of a voltage-clamp current recording

III. Noise Sources and Bandwidth Limits

A. Signal-to-Noise Ratio and Bandwidth

Sources of noise in nanopore recordings can be described by their spectral noise density $S_n(f)$, and the expected time-domain noise amplitude is a monotonically-increasing function of the measurement bandwidth. For a given signal amplitude ΔI, the signal-to-noise ratio is then a function of the measurement bandwidth, and described by:

$$SNR(B) = \frac{\Delta I}{I_{RMS(B)}} = \frac{\Delta I}{\sqrt{\int_{f_{min}}^{B} S_n(f)df}} \quad (2)$$

The appropriate definition for ΔI will depend on the goals of an experiment. In some cases it may be the entire change in ionic current that a molecule causes from the baseline, while other times it is necessary to distinguish between multiple blockade levels, requiring a smaller ΔI to be resolved.

In all cases, there will be some minimum tolerable signal to noise ratio (SNR_{MIN}), and we can define the maximum bandwidth (B_{MAX}) as the bandwidth beyond which SNR< SNR_{MIN} [4]. In the discussions that follow, we apply this concept to describe the bandwidth limitations from several important noise sources. The overall B_{MAX} will be determined by whichever noise source is the most restrictive in a given application.

B. Flicker Noise

Noise that has a power spectral density which scales as $S_n(f) \propto 1/f$ is referred to as flicker noise. Flicker noise is known to correlate with drift and offset variations, and it is particularly harmful in applications which consider long-duration signals or assume steady statistical properties over long periods of time.

Flicker noise in nanopore sensors is often characterized empirically as [9]:

$$S_n(f) = \frac{AI^2}{f} \ \text{A}^2\,\text{Hz}^{-1} \quad (3)$$

where I is the DC current and A is a normalized flicker noise coefficient.

Since flicker noise spectral density is larger at lower frequencies, in the presence of flicker noise B_{MAX} is a strong function of not only the flicker noise parameters but also the minimum required signal frequency. The maximum signal bandwidth determined by flicker noise alone is:

$$B_{MAX} \approx f_{min}\left(\exp\left[\frac{1}{AI^2}\left(\frac{\Delta I}{SNR_{MIN}}\right)^2\right] - 1\right) \ \text{Hz} \quad (4)$$

C. Johnson Noise

Real conductors, whether they are electronic resistors or ionic channels, exhibit noise due to random thermal fluctuations. This noise is named Johnson noise, and it has a constant power spectral density P(f) = 4kT W Hz^{-1}, where k is Boltzmann's constant and T is the absolute temperature. For a resistance R, this can be expressed as an equivalent noise current power spectral density, $S_n(f) = 4kT/R\ A^2\ Hz^{-1}$.

In a nanopore measurement, Johnson noise is typically introduced both through the feedback resistance R_F, and from the pore itself, R_P. Together, these form an effective thermal noise resistance $R_T = \left(\frac{1}{R_F} + \frac{1}{R_P}\right)^{-1}$, leading to a maximum bandwidth of:

$$B_{MAX} \approx \left(\frac{\Delta I}{SNR_{MIN}}\right)^2 \frac{R_T}{4kT} \ \text{Hz} \quad (5)$$

D. Shot Noise

Electronic currents are carried by discrete charged particles, and thus at a fine enough timescale all charge movements are discrete. Shot noise defines the variance of these discrete charge movements according to its power spectral density. If a constant current travels across a unidirectional barrier (such as a diode), $S_n(f) = 2qI\ A^2\ Hz^{-1}$, where q is the elementary charge and I is the current.

Nanopores themselves usually do not exhibit shot noise, but transistors in the electronics used to measure them do. Current-measurement circuits in which the signal current immediately passes through a diode or transistor, rather than a resistor, may directly contribute shot noise which scales with the nanopore bias current.

The maximum signal bandwidth determined by shot noise from a unidirectional current I is:

$$B_{MAX} \approx \left(\frac{\Delta I}{SNR_{min}}\right)^2 \frac{1}{2qI} \text{ Hz} \quad (6)$$

E. Capacitive Noise Currents

Ideal capacitors are lossless, and themselves generate no noise. However, non-ideal capacitors can contribute noise due to thermal dissipation in lossy dielectric materials, leading to a noise spectrum $S_n(f) = 8\pi fkTC_L \tan\delta$ A^2 Hz^{-1}, where C_L is a capacitance with a dielectric loss angle δ. The maximum signal bandwidth is then:

$$B_{MAX} \approx \frac{\Delta I}{SNR_{MIN}} \frac{1}{\sqrt{4\pi kTC_L tan\delta}} \text{ Hz} \quad (7)$$

Additionally, in a voltage-clamp circuit even ideal capacitors will contribute noise when paired with a noisy operational amplifier. The amplifier's equivalent input voltage noise appears across any input capacitance along with the desired bias. Thus the maximum signal bandwidth determined by the noise currents from a total capacitance C_{TOT} at the input depends on the voltage noise properties of the operational amplifier. If the amplifier exhibits flicker voltage noise ($v_n^2 = A_v/f$ $V^2 Hz^{-1}$), the noise is described by $S_n(f) = A_v(2\pi C_{TOT})^2 f$ $A^2 Hz^{-1}$ and B_{MAX} is:

$$B_{MAX} \approx \frac{\Delta I}{SNR_{MIN}} \frac{1}{\pi\sqrt{2A_v}} \frac{1}{C_{TOT}} \text{ Hz} \quad (8)$$

while if the amplifier exhibits white noise (constant v_n^2), then $S_n(f) = (2\pi f C_{TOT} v_n)^2$ $A^2 Hz^{-1}$ and the maximum bandwidth is:

$$B_{MAX} \approx \left(\frac{\Delta I\sqrt{3}}{SNR_{MIN} \times 2\pi C_{TOT} \times v_n}\right)^{\frac{2}{3}} \text{ Hz} \quad (9)$$

F. Other Noise Sources

It is, of course, possible for other sources of noise to interfere with the measurement. Electromagnetic interference and ground loops can be a significant concern if the system is not properly isolated. Later stages of electronic amplifiers and filters will add noise, as will the process of digitization. However, in a reasonably optimized system these sources should be strongly suppressed, leaving the broadband noise sources discussed above to dominate the noise floor.

IV. Electronic Systems for Nanopore Recordings

A. Commercial Patch Clamp Amplifiers

The majority of nanopore instrumentation has been inherited from patch-clamp electrophysiology setups. Voltage-clamp amplifiers such as the Axopatch 200B (Molecular Devices) and HEKA EPC-10 (HEKA Elektronik) were designed for patch-clamp recordings of ion channels, and these amplifiers produce the lowest-noise time-domain current recordings of any available commercial instruments.

Unfortunately for nanopore researchers, time-resolved recordings with patch-clamp amplifiers were primarily optimized for the < 10 pA signals produced by single ion channels in physiological conditions. Noise density at frequencies greater than 10 kHz is sacrificed in the name of higher accuracy at lower bandwidth, and the systems generally choose not to support bandwidths above 100 kHz, as in their intended applications such recordings would have unacceptably high noise amplitudes.

B. Integrated Electronics

Several integrated circuit amplifiers for nanopore and patch-clamp recordings have been reported [4, 10-13]. These integrated amplifiers are several orders of magnitude smaller than discrete patch-clamp systems, and consume considerably less power, but they often struggle to achieve noise performance competitive with discrete patch-clamp amplifiers.

One common challenge with integrated patch-clamp systems is the difficulty of designing a sufficiently low-noise on-chip feedback network, namely the element R_F (Fig. 1). High-value resistors in integrated semiconductors can be prohibitively large, nonlinear, or have high parasitic capacitances. Charge-sensitive amplifiers with purely capacitive feedback are common in other integrated preamplifiers, but nanopore sensors often have high DC bias currents which would require very frequent capacitor resets.

Other factors detrimental to the performance of integrated amplifiers are the properties of the available transistors. Discrete designs invariably use junction field-effect transistors (JFETs) as the first stage of the operational amplifier [14]. JFETs offer low gate leakage current, low white voltage noise, and low flicker noise. The integrated-circuit alternative is typically a MOS transistor, which has negligible gate current and only moderately larger white noise, but which suffers greatly when it comes to flicker voltage noise.

Despite ongoing challenges in reducing low-frequency noise sources, the miniaturization of both the electronics and fluidics promises to inherently reduce parasitic capacitances and greatly improve the high-frequency noise floor [4]. To reach their full potential, integrated nanopore amplifiers will need to be matched with similarly miniaturized fluidics. The fluid cells used for nanopore recordings are often several centimeters, compared to the sub-millimeter dimensions of integrated amplifiers. Future systems will likely require assembling arrays of isolated lipid bilayers [15], exposing microscale amplifiers directly to an electrolyte [4], or embedding solid-state nanopores into the amplifier chips themselves [16, 17].

V. Future Prospects

A. Protein Nanopore Temporal Resolution

To consider a fundamental signal-to-noise limitation for nanopore sensors, we can first imagine idealized scenarios with zero input capacitance and very high transimpedance

gain (R_F). In such a system, measurements of an α-HL nanopore would be limited only by the thermal noise floor of the ion channel. In 1M KCl, this would mean that the noise could be approximated as:

$$I_{RMS-\alpha HL-min} \approx \sqrt{\frac{4kTB}{R_P}} \approx 4fA \times \sqrt{B} \quad \text{Hz} \qquad (10)$$

which would correspond to 1.3 pA_{RMS} at B = 100 kHz, or 4 pA_{RMS} at B = 1 MHz. In theory, pulses with amplitude ΔI = 100 pA could be detected with SNR = 5 at a bandwidth greater than 20 MHz, meaning that events as brief as 25 nanoseconds would be distinguishable above the background thermal noise.

In practice, such performance is impossible due to non-zero parasitic capacitance. In the α-HL example, using a discrete patch-clamp amplifier with typical values of v_n = 3 nV Hz^{-1} and C = 10 pF, the capacitive noise exceeds the thermal noise floor for f > 22 kHz.

With existing high-performance analog semiconductor technology, a challenging goal might be to produce a measurement system with an amplifier voltage noise of 1 $nV/\sqrt{Hz}$ and 0.5 pF total capacitance. With such an amplifier, and an appropriately small-area lipid bilayer, the capacitive noise would not exceed the thermal noise of an α-HL nanopore until B > 1 MHz. If this system can be realized, pulses of ΔI = 100 pA would be detectable at SNR = 5 up to B ≈ 5 MHz. Thus it is feasible that blockades as brief as 100 ns could be resolved in protein nanopores.

B. Solid-State Nanopore Temporal Resolution

With bias current commonly an order of magnitude larger than protein nanopores, recordings of solid-state nanopores can tolerate higher noise levels and reach even finer temporal resolution. A solid-state nanopore may have a conductance on the order of 50 MΩ, which at 300 mV would provide an upper bound of ΔI = 6 pA. Considering Johnson noise alone, such a signal would be observable with SNR = 5 at bandwidths greater than 1 GHz.

Once again, parasitic capacitance would prevent this resolution from actually being reached. A reasonable estimate for the total parasitic capacitance present in many recent solid-state nanopore studies is 50 pF, while in our previous work [4] we were able to decrease the total capacitance to less than 10 pF. The capacitance of solid-state nanopore supports is often higher than their lipid membrane counterparts, but if a 1 $nV/\sqrt{Hz}$ and 0.5 pF amplifier were achieved, and the nanopore's membrane capacitance were reduced to 0.5 pF, it could be possible to measure solid-state nanopore signals with SNR > 5 at bandwidths above 40 MHz, identifying blockages that last for only 12.5 ns.

Such high signal bandwidths would be well into the regime of purely diffusive motion of small molecules, and would be even faster than the estimated velocities of freely-moving DNA through nanopores [2], relaxing the need to drastically slow down the motion of intact DNA for nanopore strand sequencing. These timescales are also directly accessible to molecular dynamics simulations [18, 19], enabling closer connections between experimental and simulated observations of dynamic single-molecule processes.

REFERENCES

[1] D. Branton, D. W. Deamer, *et al.*, "The potential and challenges of nanopore sequencing.," *Nature Biotechnology,* vol. 26, pp. 1146-53, 2008.

[2] B. M. Venkatesan and R. Bashir, "Nanopore sensors for nucleic acid analysis," *Nature Nanotechnology,* pp. 1-10, 2011.

[3] B. Sakmann, "Single-Channel Recording," 2009.

[4] J. K. Rosenstein, M. Wanunu, C. A. Merchant, M. Drndic, and K. L. Shepard, "Integrated nanopore sensing platform with sub-microsecond temporal resolution," *Nature Methods,* vol. 9, 2012.

[5] J. J. Kasianowicz, E. Brandin, D. Branton, and D. W. Deamer, "Characterization of individual polynucleotide molecules using a membrane channel.," *Proceedings of the National Academy of Sciences of the United States of America,* vol. 93, pp. 13770-3, 1996.

[6] C. Dekker, "Solid-state nanopores.," *Nature Nanotechnology,* vol. 2, pp. 209-15, 2007.

[7] M. J. Kim, M. Wanunu, D. C. Bell, and a. Meller, "Rapid Fabrication of Uniformly Sized Nanopores and Nanopore Arrays for Parallel DNA Analysis," *Advanced Materials,* vol. 18, pp. 3149-3153, 2006.

[8] M. Wanunu, T. Dadosh, V. Ray, J. Jin, L. McReynolds, and M. Drndić, "Rapid electronic detection of probe-specific microRNAs using thin nanopore sensors.," *Nature Nanotechnology,* vol. 5, pp. 807-814, 2010.

[9] R. M. M. Smeets, N. H. Dekker, and C. Dekker, "Low-frequency noise in solid-state nanopores.," *Nanotechnology,* vol. 20, p. 095501, 2009.

[10] J. Kim, R. Maitra, K. Pedrotti, and W. Dunbar, "A Patch-Clamp ASIC for Nanopore-Based DNA Analysis," *ieeexplore.ieee.org,* pp. 1-1, 2012.

[11] P. Weerakoon, E. Culurciello, Y. Yang, J. Santos-Sacchi, P. J. Kindlmann, and F. J. Sigworth, "Patch-clamp amplifiers on a chip.," *Journal of Neuroscience Methods,* vol. 192, pp. 187-92, 2010.

[12] G. Ferrari, F. Gozzini, A. Molari, and M. Sampietro, "Transimpedance Amplifier for High Sensitivity Current Measurements on Nanodevices," *IEEE Journal of Solid-State Circuits,* vol. 44, pp. 1609-1616, 2009.

[13] J. Prakash, J. Paulos, and D. Jensen, "A monolithic patch-clamping amplifier with capacitive feedback," *Journal of Neuroscience Methods,* vol. 27, pp. 165-172, 1989.

[14] F. J. Sigworth, "Electronic Design of the Patch Clamp," *Single-Channel Recording,* 2009.

[15] G. Baaken, M. Sondermann, C. Schlemmer, J. Rühe, and J. C. Behrends, "Planar microelectrode-cavity array for high-resolution and parallel electrical recording of membrane ionic currents.," *Lab on a Chip,* vol. 8, pp. 938-44, 2008.

[16] J. Rosenstein, V. Ray, M. Drndic, and K. Shepard, "Nanopore DNA sensors in CMOS with on-chip low-noise preamplifiers," *Solid-State Sensors, Actuators, and Microsystems (Transducers),* pp. 874-877, 2011.

[17] A. Uddin, S. Yemenicioglu, C.-H. Chen, E. Corigliano, K. Milaninia, and L. Theogarajan, "Integration of solid-state nanopores in a 0.5 µm CMOS foundry process.," *Nanotechnology,* vol. 24, p. 155501, 2013.

[18] J. L. Klepeis, K. Lindorff-Larsen, R. O. Dror, and D. E. Shaw, "Long-timescale molecular dynamics simulations of protein structure and function.," *Current opinion in structural biology,* vol. 19, pp. 120-7, 2009.

[19] A. Aksimentiev, "Deciphering ionic current signatures of DNA transport through a nanopore," *Nanoscale,* vol. 2, p. 468, 2010.